



CASE STUDY // RAILWAY INDUSTRY

## MODEL CALIBRATION OF A RAILWAY VEHICLE

With the help of optiSlang, calibration of a numerical model of Alfa Pendular train, including the car body, bogies and passenger-seat system, was conducted based on the natural frequencies and modal configurations estimated from dynamic tests.

### Optimization task

When interacting with the railway track, moving trains induce vibrations that can affect the structural stability of the infrastructure, the stability of the track and of the wheel-rail contact and passengers' comfort. Complex models of the train-track coupled system are developed in order to perform an accurate analysis of the dynamic behaviour. In this type of models the modelling of the vehicles is conducted based on formulations grounded on the multi body dynamics and on formulations based on the finite-element method. In formulations based on the multi body dynamics, the car body, bogies and axles of the vehicles are modelled through rigid structures connected by springs and dampers which simulate the primary and secondary suspensions. In formulations based on the finite-element method it is possible to consider the deformability of the car body, bogies and axles. The development of these models requires the knowledge of the geometrical and mechanical parameters of the vehicle's structure.

The use of models which consider the deformability of the car body of the vehicle becomes more important due to the tendency to use increasingly lighter and slender structures

in the manufacture of trains to reduce weight and construction costs. It has been shown that the flexural vibration of the car body may contribute, in a large extent, to the accelerations that passengers are subjected to. The frequencies of these vibration modes range from 8.5 Hz to 13 Hz, which is significantly relevant regarding human beings' sensitivity to vibration.

This article describes the calibration of a numerical model of an Alfa Pendular train vehicle base on modal parameters. The modal parameters of the vehicle were determined based on a set of forced vibration tests that focused specifically on the car body, bogie and passenger-seat system. The calibration of the numerical model was conducted using a multistep approach involving two phases: the first phase concerned the calibration of the model of the bogie and the second phase focused on the calibration of the complete model of the vehicle. The calibration methodology involved a sensitivity analysis and an optimization. The global sensitivity analysis was based on a stochastic sampling technique and allowed the identification of the numerical parameters that most affect the modal responses

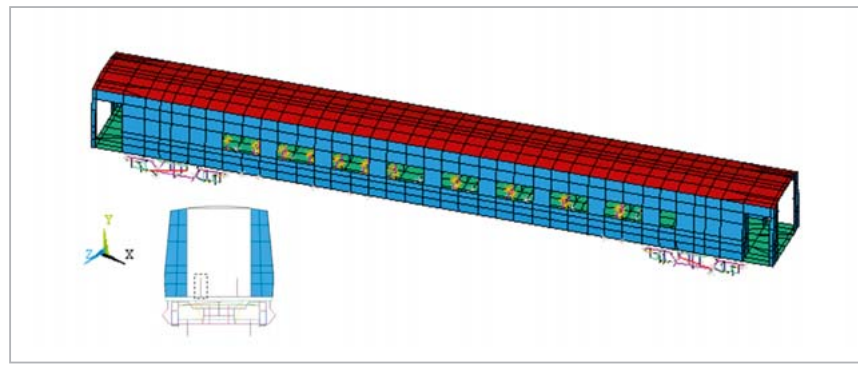


Fig. 1: Numerical model of the BBN vehicle

and, therefore, should be included in the optimization of the model. The optimization was carried out based on an iterative procedure using a genetic algorithm. A mode pairing criterion based on the modal strain energy using the Enhanced Modal Assurance Criterion (EMAC) was used to achieve the correct pairing of the numerical and experimental vibration modes. Finally, the modal parameters of the calibrated numerical model are compared with the modal parameters of the initial numerical model.

### Numerical modelling

#### Description

The modal analysis of the BBN vehicle was performed using a three-dimensional finite element model developed in the ANSYS software. The use of a finite-element formulation allows considering the influence of the deformability of the car body, bogies and axles. Figure 1 presents a perspective of the numerical model. The car body was modelled by shell-finite elements while the bogies were modelled by beam-finite elements, with the exception of the suspensions, the connecting rods and the tilting system which were modelled by spring-damper assemblies. Additionally, the passenger-seat system was modelled, in a simplified manner, by a one-DOF system composed of a mass over a spring-damper assembly. The masses of the equipment located in the under-floor of the car body and bogies were simulated through mass elements. The structure was discretised with 1082 shell elements, 1029 beam elements and 148 spring-damper assemblies. The total number of nodes is 1902, corresponding to 10,704 degrees of freedom.

#### Car body

Table 1 presents the main geometric and mechanical parameters of the car body's numerical modelling, including the designation, the selected value, the unit and the bibliographic references that were used. Additionally, the characteristics of the statistical distribution of some of the parameters, later used in the calibration phase of the model are also shown. Figure 2 identifies the panels of finite elements considered in the numerical modelling of the car body in correspondence with the base, cover and side walls. In the

modelling of the side walls special attention was given to the positioning of openings corresponding to windows and access doors. The finite elements that simulate the various panels have length  $l$  and constant thickness  $e$  and are constituted by elastic and orthotropic materials. The thickness of each panel was determined based on the condition that the cross-sectional area of the

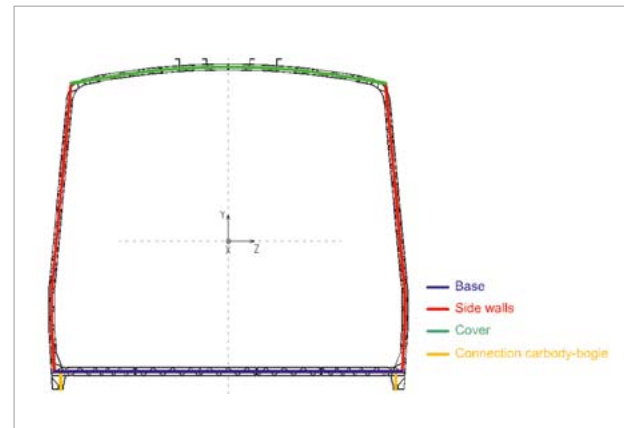


Fig. 2: Finite-elements panels from the numerical modelling of the carbody

finite-element panel is equal to the cross-sectional area of the real panel. The inertia correction of the panels, in directions  $x$  and  $z$ , was performed using the RMI parameter (Ratio of the bending Moment of Inertia):

$$RMI = \frac{I_{real}}{I_{mod}}$$

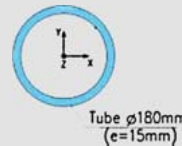
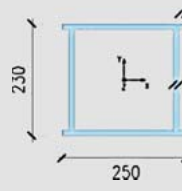
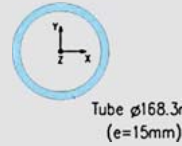
in which  $I_{real}$  is the real inertia of the panel and  $I_{mod}$  is the inertia calculated based on the thickness of the shell-finite element. The additional masses of the base, side walls and cover of the car body refer to the mass parcels of the item others under the component equipment and were uniformly distributed on the surface of the respective structural elements. The stiffness and damping parameters of the secondary suspension elements as well as their respective variation limits were estimated based on the values provided by the train's manufacturer.

#### Bogie

Figure 3 (see page 22) presents a perspective of the numerical model of the bogie. The chosen colours, combined with the legend, facilitate the identification of the different elements of the bogie. The beam elements connecting the wheel sets to the axle box have zero stiffness around their axle, so as to simulate the linkage with the axle box. The support conditions imposed on the bogie, particularly on

Parameter	Designation	Type	Statistical distribution		Adopted value	Unit	
			Average value/ standard deviation	Limits (lower/upper)			
$K_{S1}$	Stiffness of the vertical secondary suspension	Front bogie	Uniform	256.4/7.5	247/272.9	256.4	kN/m
$K_{S2}$		Rear bogie					
$c_s$	Vertical secondary suspension damping	Uniform		35/3.0	29.8/40.3	35	kN s/m
$c_{AL}$	Yaw suspension damping	Uniform		400/34.6	340/460	400	kN s/m
$K_b$	Stiffness of the tilting bolster-load bolster connection rod	Uniform		20,000/8660	5000/35,000	20,000	kN/m
$\rho_{alum}$	Aluminium density	-	-	-/-	-/-	2700	kg/m <sup>3</sup>
$E$	Modulus of deformability of aluminium	-	-	-/-	-/-	70	GPa
$RMI_b$	Corrective factor of the moment of inertia	Base	Uniform	225/101	50/400	90	-
$RMI_p$		Side walls	Uniform	90/34.6	30/150	114	-
$RMI_c$		Cover	Uniform	300/57.7	200/400	386	-
$\Delta Mb$	Additional mass	Base	Uniform	70/11.5	50/90	70	%
$\Delta Mp$		Side walls	Uniform	20/8.7	5/35	20	%
$\Delta Mc$		Cover	Uniform	7.5/4.3	0/15	10	%
$e_{bas}$	Equivalent thickness	Base	-	-/-	-/-	10.2	mm
$e_{par}$		Side walls	-	-/-	-/-	10.3	mm
$e_{cob}$		Cover	-	-/-	-/-	8.8	mm

Tab. 1: Characterisation of the main parameters of the numerical model of the carbody

Element	Cross-section	Geometrical characteristics
Axle		$A = 0.00778 \text{ m}^2$ $I_x = 0.267 \times 10^{-4} \text{ m}^4$ $I_y = 0.267 \times 10^{-4} \text{ m}^4$ $I_z = 0.534 \times 10^{-4} \text{ m}^4$
Girder (central zone)		$A = 0.01093 \text{ m}^2$ $I_x = 0.857 \times 10^{-4} \text{ m}^4$ $I_y = 0.887 \times 10^{-4} \text{ m}^4$ $I_z = 0.121 \times 10^{-3} \text{ m}^4$
Crossbar		$A = 0.00718 \text{ m}^2$ $I_x = 0.210 \times 10^{-4} \text{ m}^4$ $I_y = 0.210 \times 10^{-4} \text{ m}^4$ $I_z = 0.421 \times 10^{-4} \text{ m}^4$

Tab. 2: Geometric characteristics of the structural elements of the bogies

the girders and on the tilting and load bolsters, allow translational vertical movements and rotations around the  $x$  and  $z$  axes, preventing any other movements. Table 2 shows the geometrical characteristics of the sections of the various elements. The geometric characteristics are expressed in terms of the area ( $A$ ) and inertias ( $I$ ). Table 3 (see page 22) describes the main mechanical and geometrical parameters of the numerical model and the characteristics of the statistical distribution of certain parameters, which will be used in the model's calibration phase.

The stiffness and damping parameters of primary suspension elements and their respective variation limits were estimated based on information from the manufacturer. The additional mass of the bogie, at the girders, crossbars and axles, is related to the mass of springs, dampers, connecting rods, links, reinforcement plates, axle boxes and others. These masses were linearly distributed in the different elements. In what concerns the girders the additional mass was further divided into two parcels according to their location: in the central zone, i.e. in the sections located between the cross-bars and at the extremities. The wheel-rail connection was modelled by a spring element with unidirectional behaviour.

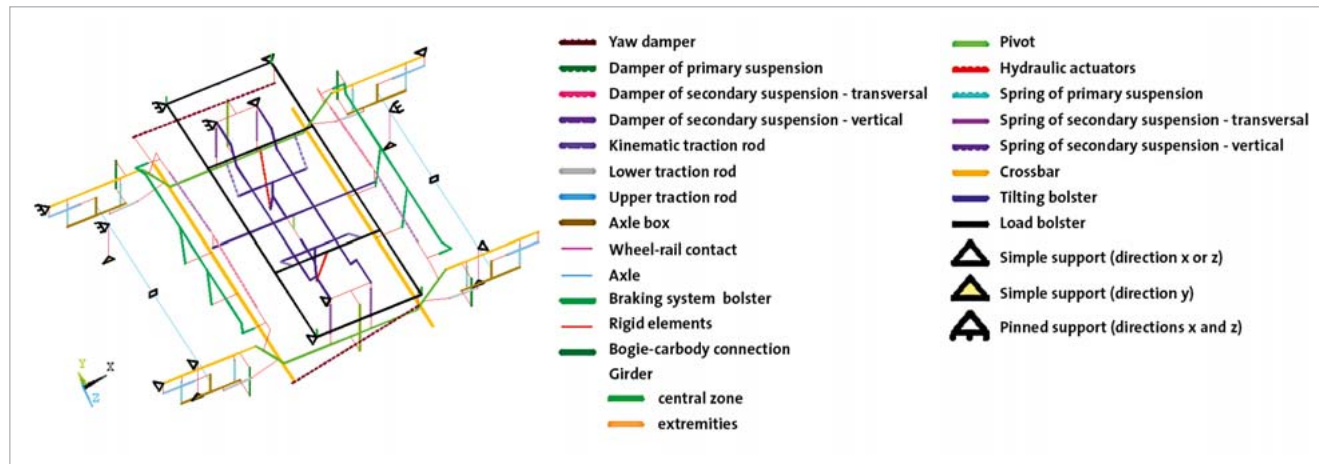


Fig. 3: Numerical model of the bogie

Parameter	Designation	Type	Statistical distribution		Adopted value	Unit
			Average value/ standard deviation	Limits (lower/upper)		
$K_p$	Stiffness of the primary suspension	Uniform	564/26.6	518/610	564	kN/m
$c_p$	Damping of the primary suspension	Uniform	18/1.6	15.3/20.7	18	kNs/m
$K_{bls}$	Stiffness of the axle box connecting rods	Upper	6.5/0.8	5.2/7.8	6.5	MN/m
$K_{bli}$		Lower	25/2.9	20/30	25	MN/m
$K_{rc}$	Stiffness of the wheel-rail connection	-	-/-	-/-	$1.5674 \times 10^9$	mN/m
$\Delta Mlc$	Additional-mass	Girder (central area)	75/43.3	0/150	42	kg/m
$\Delta Mle$		Girder (extremities)	30/17.3	0/60	38	kg/m
$\Delta Mt$		Crossbar	125/72.2	0/250	92	kg/m
$\Delta Me$		Axles	-	-/-	-/-	271

Tab. 3: Characterisation of the main parameters of the numerical model of the bogie

Element	Mode	Nature of vibration mode	Damped frequency (Hz)	Undamped frequency (Hz)	
Carbody	1C	Rigid body	Rolling	0.86	0.82
	2C		Bouncing	1.04	1.00
	3C		Pitching	1.42	1.33
	4C	Structural	First distortion	10.21	10.21
	5C		First bending	16.20	16.20
	6C		First torsion	15.05	15.03
Bogies	1B	Rigid body	Bouncing	8.21/8.18	6.57/6.26
	2B		Rolling	4.89/5.28	4.09/4.53
	3B		Pitching	12.10/12.04	9.50/9.41

Tab. 4: Numerical natural frequencies of the carbody and bogies

**Modal parameters**

Table 4 shows the damped and undamped natural frequencies of the main vibration modes of the BBN vehicle. In what concerns the bogies, for modes 1B and 2B, there are different frequency values according to the movement of the two bogies in phase and in antiphase, respectively. In the 3B mode, the different values of the frequencies are related to the isolated movements of the left and right bogies, respectively. The modal results show differences between damped and undamped natural frequencies. These differences are more notorious for the rigid body modes of the car body and bogies since these modes involve significant movements of the suspensions. In case of the bogies the differences are even more important since this additional damping is provided simultaneously by the primary and secondary suspensions. Figure 4 illustrates the modal configurations associated with rigid body modes (1C, 2C and 3C) and structural modes of distortion (4C), bending (5C) and torsion (6C) of the car body. In these modes the movements of the bogie have very low amplitude. Figure 5

shows the modal configurations, in perspective and cross-section view, of a bogie of the vehicle. Mode 1B comprises the bouncing movement of the bogie. Modes 2B and 3B comprise the rolling and pitching movements of the bogie, respectively. In these modes the car body shows very limited movements.

**Calibration methodology**

The results of the conducted experimental tests of the BBN vehicle involving the dynamic tests of the car body, bogie and passenger-seat system are used to calibrate the numerical model of the vehicle. The calibration of the numerical model of the BBN vehicle was performed using an iterative method based on an optimisation technique. This method consists on the resolution of an optimisation problem, which consists of the minimisation of an objective function by varying a set of the preselected model parameters. The pre selection of the numerical parameters is carried out based on a global sensitivity analysis. Figure 6 (see page 24) presents a flow-



Fig. 4: Numerical rigid body and structural modes of vibration of the carbody

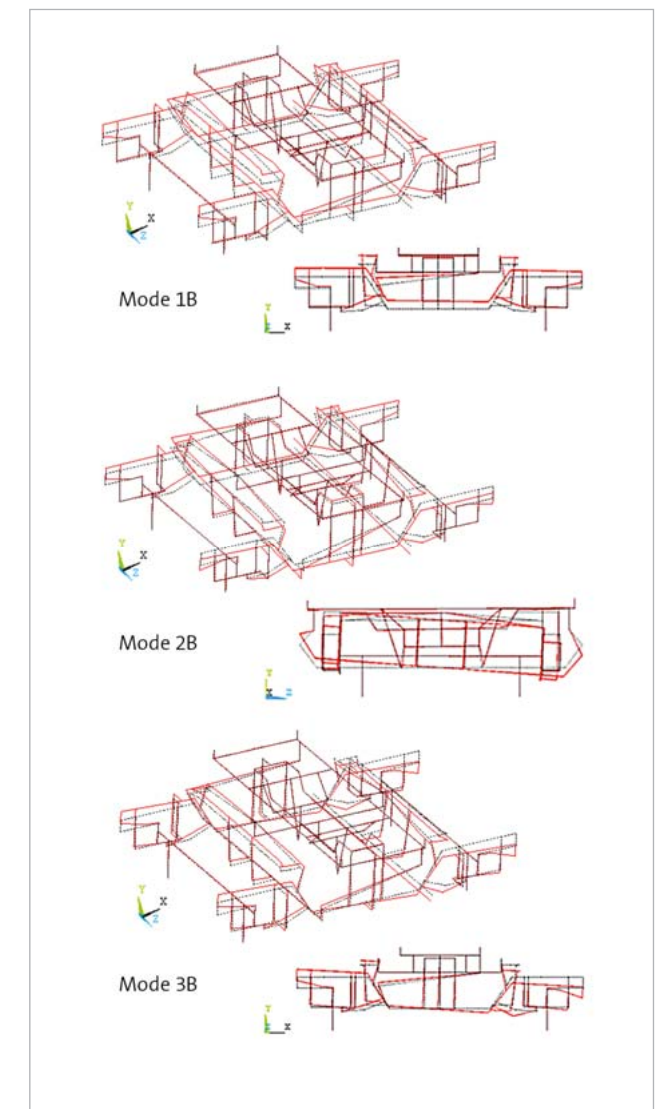


Fig. 5: Numerical modes of vibration of the bogies

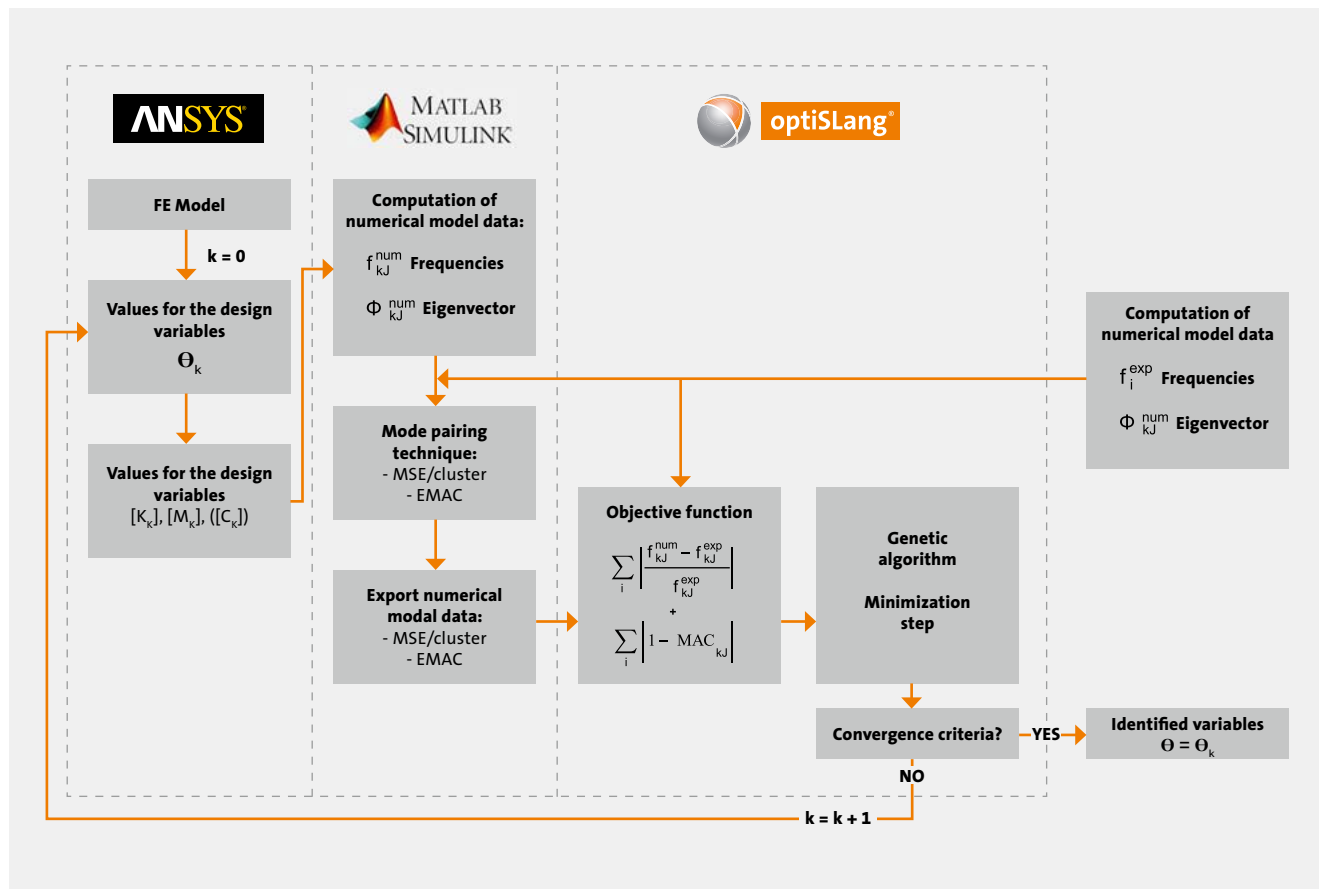


Fig. 6: Calibration methodology for the numerical model

chart illustrating the iterative method of calibration based on a genetic algorithm involving the use of three software tools: ANSYS, MATLAB and optiSLang. The main aspects of the implemented calibration methodology are described in reference. The calculation of modal parameters in systems with proportional damping matrix is based on a classic modal analysis [1]. In systems with non-proportional damping matrix the same calculation is based on a state-space formulation. The mode-pairing technique aims to establish a correspondence between experimental and numerical vibration modes. This task is often complex due to alterations in the order of the numerical modes, resulting from variations on the numerical parameters which occur during the optimisation process and also due to the limited number of degrees of freedom of experimental modes, which increases the number of possible correspondence between numerical and experimental modes. In this paper the correspondence between numerical and experimental modes is performed through an energetic criterion based on the modal strain energy and on the EMAC parameter. The objective function ( $f$ ) is defined based on the differences between the numerical and experimental modal parameters [1]:

$$f = a \sum_{i=1}^n \left| \frac{f_i^{\text{exp}} - f_i^{\text{num}}}{f_i^{\text{exp}}} \right| + b \sum_{i=1}^n |\text{MAC}(\varphi_i^{\text{exp}}, \varphi_i^{\text{num}}) - 1|$$

where  $f_i^{\text{exp}}$  and  $f_i^{\text{num}}$  are the experimental and numerical frequencies referring to mode  $i$ ,  $\varphi_i^{\text{exp}}$  and  $\varphi_i^{\text{num}}$  are the vectors containing the experimental and numerical modal information related to mode  $i$ ,  $a$  and  $b$  are weighting factors of the objective function terms and  $n$  is the total number of vibration modes.

### Calibration

The experimental calibration of the numerical model of the BBN vehicle was performed based on modal parameters which were identified by the dynamic tests of the bogie and car body. The first phase focused on the calibration of the numerical model of the bogie under test conditions [1]. The second phase focused on the calibration of the complete numerical model of the vehicle. The numerical parameters of the bogie estimated in the first phase were assumed as deterministic parameters in the second phase.

### Calibration of the bogie

#### Numerical model under test conditions

The calibration of the numerical model of the bogie forced the development of a model that would reproduce the specific conditions of the test. Changes to the original model involved the removal of springs and dampers from the secondary sus-

Parameter	Designation	Type	Statistical distribution		Adopted value	Unit	
			Average value/standard deviation	Limits (lower/upper)			
$K_b$	Stiffness of the secondary suspension's elastic block	Dir $y^a$	Uniform	12,000/1732	9000/15,000	12,000	kN/m
$K_{btl}$		Dir $x$ and Dir $z^a$	Uniform	25,250/14,289	500/50,000	5000	kN/m
$Pos_{le}$	Position of the contact point of the actuation system	Dir $x^a$ Left side	Uniform	5/1.7	2/8	5	-
$Pos_{ld}$		Right side					
$Pos_{te}$		Dir $z^a$ Left side	Uniform	0/0.6	-1/1	0	-
$Pos_{td}$		Right side					
$E_m$	Modulus of deformability of wood	Uniform		8/2.3	4/12	10	GPa

Tab. 5: Characterisation of the parameters of the numerical model of the bogie under test conditions (\*According to the referential of Fig.: 8)

pensions and from the tilting and load bolsters. Elements were also added to simulate the interface between the bogie and the actuation system, including distribution blocks and elastic blocks of the secondary suspensions. Rigid supports were introduced, at the contact point of the hydraulic actuators, with the ability to assume different positions, thus meeting the deviations of the contact point in the longitudinal ( $x$ ) and transverse ( $z$ ) directions. The elastic blocks of the suspension were modelled by spring elements positioned in the vertical direction. The stiffness of the contact between distribution blocks and elastic blocks of the suspension was also modelled, in the  $x$  and  $z$  directions, through spring elements. Table 5 describes the mechanical and geometrical parameters of the numerical. These parameters should be considered together with the parameters indicated in Table 3.

The position of the contact point with the actuation system, in longitudinal and transverse directions, may assume different values for the left and right hydraulic actuators. The longitudinal position of the actuator was limited to positions 2–8.

#### Sensitivity analysis

Figure 7 shows the results of the global sensitivity analysis using Spearman's rank correlation coefficient. This sensitivity analysis was performed using a stochastic sampling technique based on 500 samples generated by the Latin Hypercube method. This analysis was based on the parameters intervals presented in Tables 3 and 5. The correlation coefficients between  $[-0.25, 0.25]$  were excluded from the graphical representation. The random generation of samples, particularly the parameters of the bogie's additional mass, was subject to the following restrictions:

$$-\varepsilon \leq \Delta M - [L_{lc} \Delta M_{lc} + L_{le} \Delta M_{le} + L_t \Delta M_t] \leq \varepsilon$$

where  $\Delta M$  equals 842 kg, and  $L_{lc}$ ,  $L_{le}$  and  $L_t$  represent the total length of the central area of the girders, the extremities of the girders and crossbars, equal to 4.46 m, 3.56 m and 5.26 m, respectively, and  $\varepsilon$  is a tolerance considered equal to 150 kg.

The correlation matrix shows that the stiffness of the primary suspensions, the additional mass of the girders (central area and extremities) and the stiffness of the lower traction rod of the axle box have significant influence over

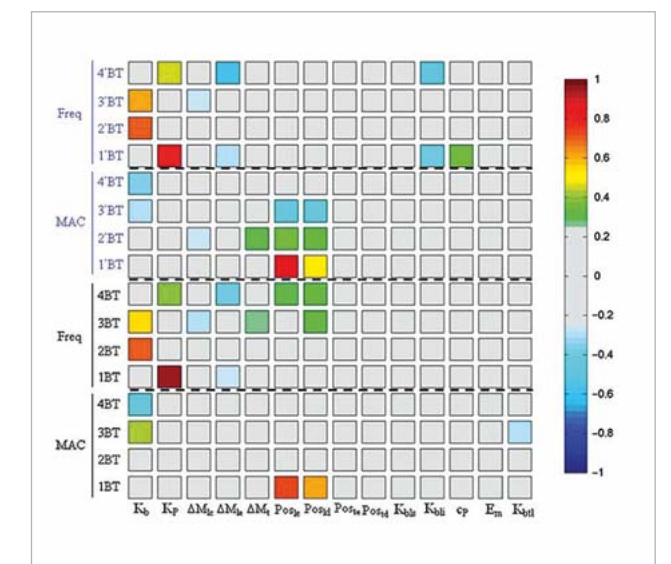


Fig. 7: Spearman's rank correlation coefficient between the parameters and responses of the numerical model of the bogie under test conditions

the vibration frequencies. In turn, the position of the actuators affects MAC values, particularly in modes 1BT. The vertical stiffness of the secondary suspension blocks influ-

ences the vibration frequencies and also the MAC values in a significant way. The remaining analysed parameters do not have significant influence on the modal responses and were therefore excluded from the optimisation phase. The influence of the primary suspensions' stiffness over the frequencies of modes 1BT and 4BT, for which the distance between the suspensions and the rotation axle of the bogie is larger, should be emphasised. In these modes the elastic block of the suspension has no influence over the responses due to its location near the rotation axle. It is not the case of the frequencies of modes 2BT and 3BT, which involve transverse translation and rotation of the bogie, respectively, and for which the stiffness of the suspension blocks, compared with the primary suspensions, is decisive for controlling the responses.

**Optimisation**

The optimisation of the model involved finally 10 numerical parameters and 16 modal results (8 vibration frequencies and 8 MAC values). The genetic algorithm was based on an initial population of 30 individuals considering 250 generations, in a total of 7500 individuals. The initial population was randomly generated by the Latin Hypercube method. A number of elites equal to 1 and a number of substitute individuals also equal to 1 have been defined in this algorithm. The crossover rate was assumed to be 50% and the mutation rate was considered equal to 15% with a standard deviation variable along the optimisation between 0.10 and 0.01.

The objective function is identical to that shown on page 24 considering a total number of vibration modes equal to 8 and weighting factors a and b equal to 1. The optimisation problem still includes restrictions related to the parameters of additional mass of the bogie. Optimal values of the parameters were obtained from the results of four independent optimisation cases (GB1–GB4) based on different initial populations. Figure 8 shows the ratios of the values of each parameter of the model in relation to the limits indicated in Tables 1, 3 and 5. The limits of the distributions of some of the parameters were extended, such as the cases of the stiffness of the primary suspension (500/1000 kN/m), and the stiffness of the axle box's traction rods (3/10 and 10/40MN/m) due to the systematic tendency of the optimum solutions of these parameters to reach the limits indicated in Table 3. A 0% ratio means that the parameter coincides with the lower limit. A ratio of 100% means that it coincides with the upper limit. The stiffness and damping parameters of the primary suspension and increments of mass are presented in Figure 8a indicating, in brackets, the numerical parameters' values.

The parameters related to the elastic elements (blocks and rod) and actuation system is shown in Figure 8b. The analysed parameters present a good stability with variations below 10%, except for the damping of the primary damper. This is one of the parameters that the sensitivity analysis has shown to have a smaller influence over the numerical

responses. Figure 9 summarises the error values between the numerical and experimental vibration frequencies, taking as reference the average values of the experimental frequencies, and the values of the MAC parameter, before and after calibration. The results after calibration are related to optimisation case GB2, which was the one presenting the lowest residual of the objective function. The average error of the frequencies decreased from 10.6% before calibration to 0.8% after calibration. In turn, the average value of the MAC parameter increased from 0.894 before calibration to 0.953 after calibration. As visualised in Figure 10, the experimentally obtained and numerically derived optimised modal configurations of the bogie coincide almost perfectly.

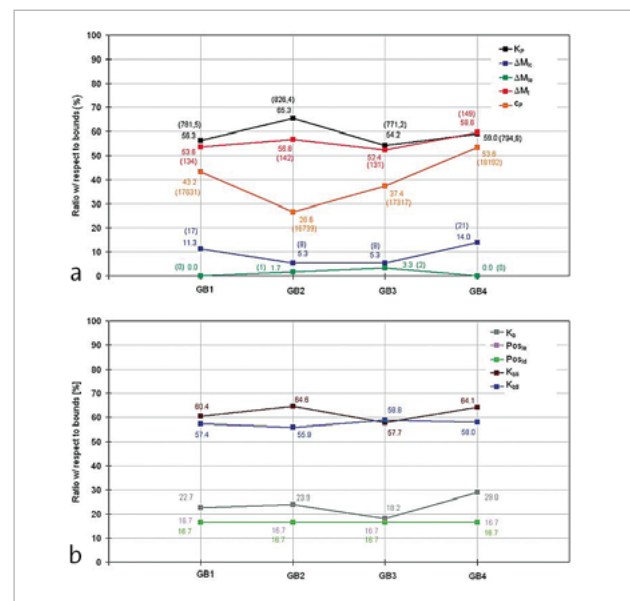


Fig. 8: Values of numerical parameters for optimisation cases GB1–GB4: (a) stiffness and damping of the primary suspension and increment of masses; (b) characteristics of the elastic elements and actuation system

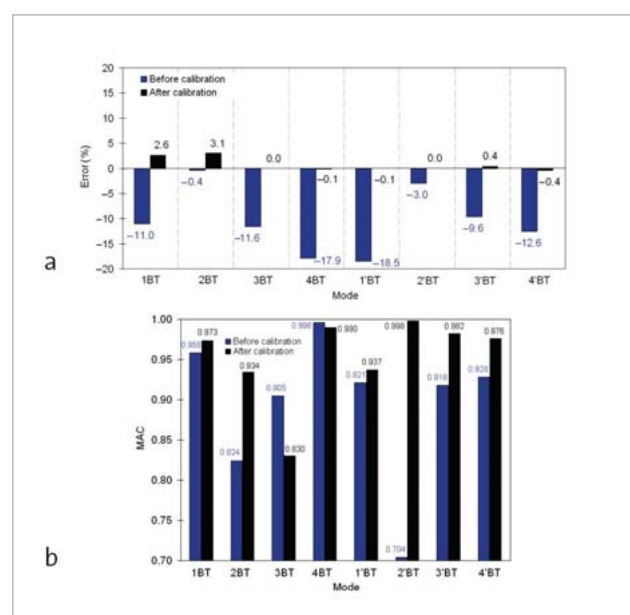


Fig. 9: Comparative analysis of the errors of experimental and numerical responses, before and after calibration: (a) vibration frequencies; (b) MAC

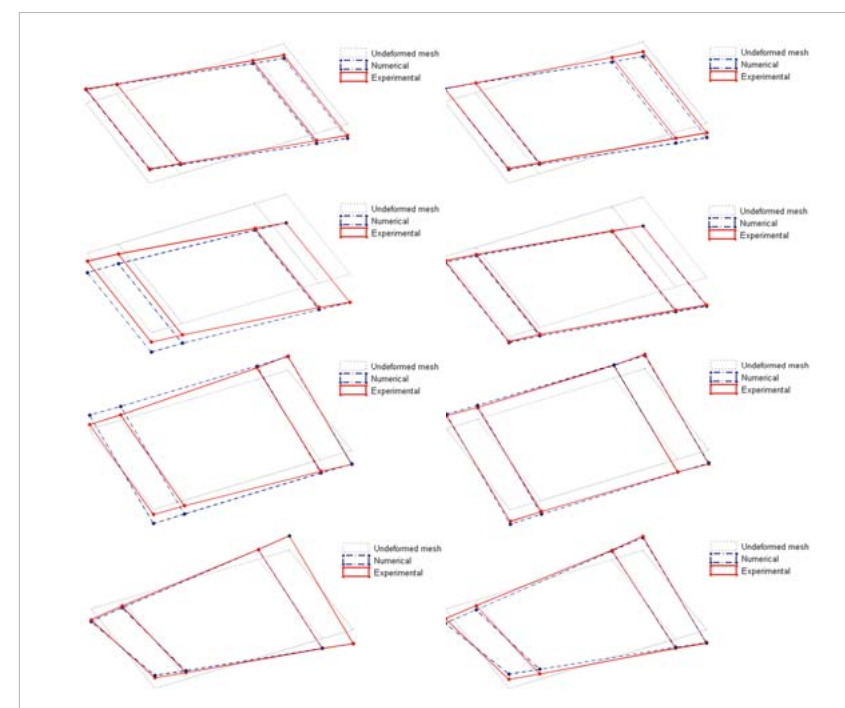


Fig. 10: Comparison between the experimental and numerical vibration modes of the bogie after calibration

**Calibration of the complete model of the BBN vehicle**

**Sensitivity analysis**

Figure 11 presents the results of the global sensitivity analysis using Spearman's rank correlation coefficient. The sensitivity analysis was performed using a stochastic sampling technique based on 250 samples generated by the Latin Hypercube method. This analysis was based on the parameters intervals presented in Table 2. The random generation of samples, particularly for the parameters of the car body's additional mass, was subject to the following restrictions:

$$-\epsilon \leq \Delta M - [L_{lc} \Delta M_{lc} + L_{le} \Delta M_{le} + L_t \Delta M_t] \leq \epsilon$$

where  $\Delta M$  and  $L_t$  represent the additional mass on the base, side walls and cover, respectively, and  $\epsilon$  is a tolerance equal to 10%. The mode pairing was performed by application of a technique based on the modal strain energy and on the EMAC parameter. The correlation matrix shows that the stiffness of secondary suspensions, from front (KS1) and rear (KS2) bogies, has significant influence over the frequencies and MAC values of the rigid body modes of the car body. In turn, the RMI parameters from the base (RMib) and side walls (RMip) essentially control the frequencies and MAC values of the structural modes of the car body. The parameters additional mass and stiffness of the connecting rod between the tilting and load bolsters (Kb) have significant influence over the vibration frequency of mode 1C. The remaining analysed parameters did not have significant influence with respect to the modal responses, and were consequently excluded from the optimisation phase.

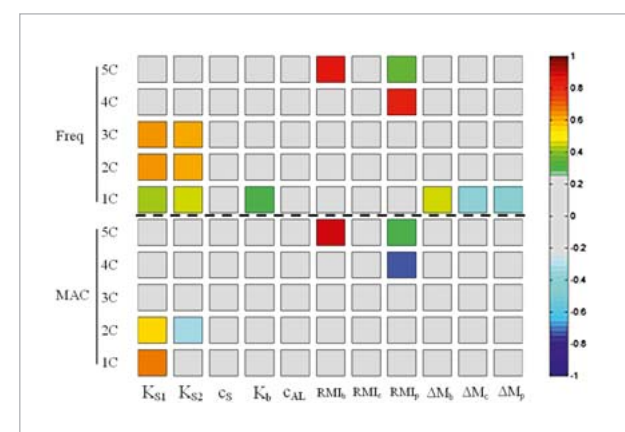


Fig. 11: Spearman's rank correlation coefficient between the parameters and responses of the carbody's numerical model

It is noticeable that the most stable parameters, with variations below 10%, are those that most affect the responses, including the stiffness of secondary suspensions and RMI

parameters of the base and side walls. The stiffness values of the front bogie's secondary suspension are higher than those estimated for the rear bogie. Regarding the additional masses of the side walls and cover, the estimates show higher variations, close to 25%. This should be related to the fact that these parameters contribute in a similar way to the participant mass on vibration mode 1C. Therefore, there may be different combinations of these parameters leading to the same solution, in terms of optimisation of the problem. Figure 13 summarises the error values of the numerical and experimental vibration frequencies taking as reference the average values of the experimental frequencies, and of the MAC parameter, before and after calibration. The results after calibration are related to the GC1 optimisation case, which was the one with the lowest final residual of the objective function. The frequencies' average error dropped from 20.3%, before calibration, to 2.9%, after calibration. This error decrease is mainly due to the reduction of the error associated with the frequencies of structural modes 4C and 5C. The average value of the MAC parameter did not change significantly, increasing from 0.927, before calibration, to 0.937, after calibration. The excellent agreement between the car body's experimentally obtained and numerically derived optimised modal configurations can be verified in Figure 14.

**Final results**

The combination between the numerical parameters, obtained for the optimisation case of the bogie GB2, and the parameters obtained in optimisation case of the complete vehicle GC1, were the basis for the establishment of the vehicle's calibrated numerical model. Table 7 presents the values of the damped vibration frequencies of the main vibration modes of the BBN vehicle obtained from the calibrated numerical model. Comparing the values of the frequencies with the values given in Table 4, concerning the initial numerical model, there is a visible tendency towards the frequency increase on the rigid body modes of the car body and bogies, being that, in the bogies' case, this increase ranged from 10% to 55%. This tendency is due to the significant increase of the stiffness of the primary and secondary suspension springs. In turn, the structural modes of the car body, particularly modes 4C and 5C showed a decreased tendency of approximately 20%, mainly due to the reduction of the RMI parameter of the car body's side walls.

**Conclusions**

This article described the calibration of the numerical model of a BBN vehicle of the Alfa Pendular train based on modal parameters. The calibration of the numerical model was conducted through an iterative methodology based on an optimisation algorithm and was performed using a multistep approach involving two phases: the first phase focused on the calibration of the model of the bogie under

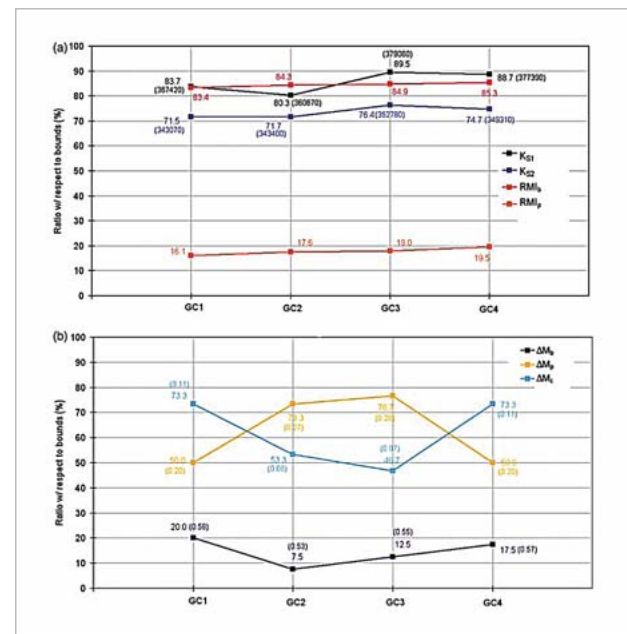


Fig. 12: Values of numerical parameters for optimisation cases GC1–GC4: (a) characteristics of the suspension, connecting rods and geometrical properties of the carbody; (b) masses

test conditions and the second focused on the calibration of the complete model of the vehicle. Global sensitivity analysis allowed the identification of numerical parameters to be considered in the calibration. The parameters that have shown the highest sensitivities in relation to the modal responses were, for the bogie, the vertical stiffness

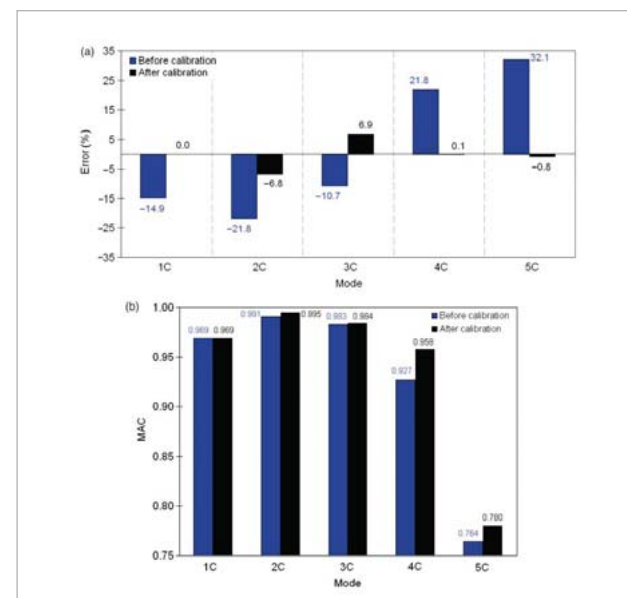


Fig. 13: Comparative analysis of the errors from the experimental and numerical responses, before and after calibration in terms of: (a) vibration frequencies; (b) MAC

of the secondary suspension block and the vertical stiffness of the primary suspensions. As for the car body, the RMI parameters of the base and side walls and the vertical stiffness of the secondary suspension were the parameters with highest sensitivity in relation to the modal responses.

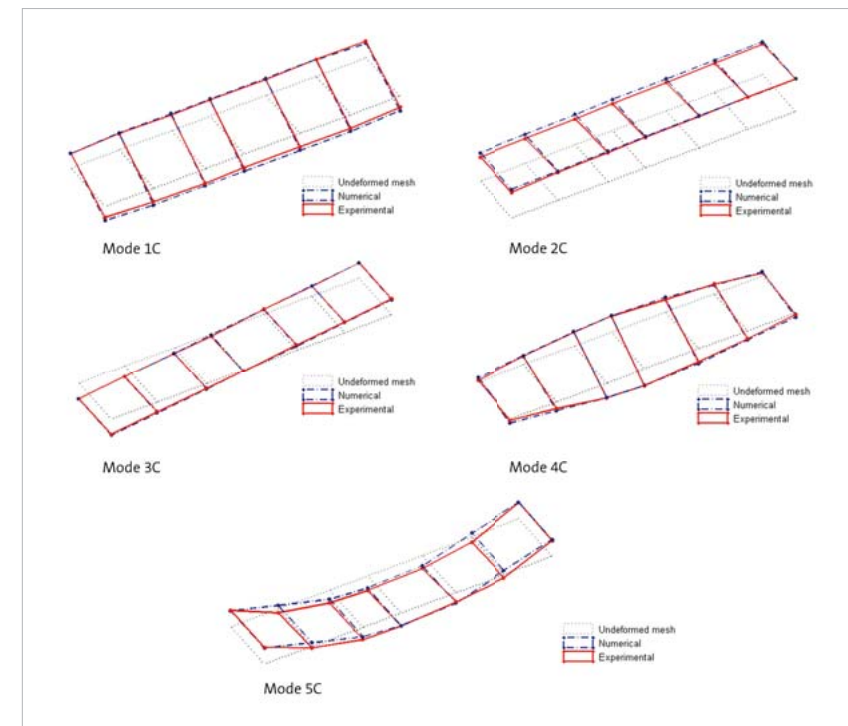


Fig. 14: Comparison between the vibration modes of the carbody, experimentally and numerically obtained, after calibration

The optimisation was conducted using a genetic algorithm involving a total of 17 numerical parameters and 26 modal responses. The results of the optimisation cases of the bogie and vehicle, based on different initial populations, led

Element	Mode	Damped frequency (Hz)
Carbody	1C	1.01
	2C	1.24
	3C	1.70
	4C	8.39
	5C	12.16
Bogies	1B	9.21/9.24
	2B	7.70/8.12
	3B	14.16/14.09

Tab. 7: Natural frequencies of the BBN vehicle obtained from the calibrated numerical model

mostly to very stable numerical parameters' values, particularly for those highly correlated with the responses. The comparison between the numerical vibration frequencies' values, before and after calibration, and the experimental vibration frequencies, has revealed significant improvements on the initial numerical models. The average error of vibration frequencies of the modes of the bogie under test conditions went from 10.6%, before calibration, to

0.8%, after calibration. Concerning the vibration modes of the complete model of the vehicle, the average error of frequencies went from 20.3%, before calibration, to 2.9% after calibration. Significant improvements were also observed in MAC values, particularly in the vibration modes of the bogie. This result demonstrates the robustness and efficiency of genetic algorithms on the estimation of the vehicle's modal responses. The combination of numerical parameters obtained for the GB2 bogie optimisation case with the parameters obtained for the GC1 case of vehicle optimisation provided the basis for developing the calibrated numerical model of BBN vehicle. Compared with the initial numerical model, the calibrated numerical models show higher frequency values of the rigid body modes of the car body and bogies, essentially due to the increased

stiffness of the primary and secondary suspension springs. On the other hand, most of the car body's structural modes tended to decrease, largely due to a reduction of the RMI parameter of the side walls of the vehicle's car body. In future studies, the calibrated numerical model of the vehicle will be used to access the dynamic behaviour of the train-track coupled system, in terms of passengers comfort and wheel-rail contact stability, on plain track, on bridges or on transition zones.

**Authors //** D. Ribeiro (School of Engineering, Polytechnic of Porto) / R. Caçada, R. Delgado ( Faculty of Engineering, University of Porto) / M. Brehm (BATir – Structural and Material Computational Mechanics, Université Libre de Bruxelles)/ V. Zabel (Bauhaus-University Weimar)

**References //** [1] D. Ribeiro, R. Caçada, R. Delgado, M. Brehm and V. Zabel (2013) - "Finite element model updating of a railway vehicle based on experimental modal parameters", *Vehicle System Dynamics*, 51 (6), pp. 821-856.

**Source //** www.dynardo.de/en/library

**Title Image //** Nuno Morão (© Wikimedia Commons)